JCTC Journal of Chemical Theory and Computation

ARTICLE

pubs.acs.org/JCTC

Use of Direct Dynamics Simulations to Determine Unimolecular Reaction Paths and Arrhenius Parameters for Large Molecules

Li Yang, Rui Sun, and William L. Hase*

Department of Chemistry and Biochemistry, Texas Tech University, Lubbock, Texas 79409, United States

ABSTRACT: In a previous study (*J. Chem. Phys.* **2008**, *129*, 094701) it was shown that for a large molecule, with a total energy much greater than its barrier for decomposition and whose vibrational modes are harmonic oscillators, the expressions for the classical Rice−Ramsperger−Kassel−Marcus (RRKM) (i.e., RRK) and classical transition-state theory (TST) rate constants become equivalent. Using this relationship, a molecule's unimolecular rate constants versus temperature may be determined from chemical dynamics simulations of microcanonical ensembles for the molecule at different total energies. The simulation identifies the molecule's unimolecular pathways and their Arrhenius parameters. In the work presented here, this approach is used to study the thermal decomposition of $CH_3-NH-CH{=}CH-CH_3$, an important constituent in the polymer of cross-linked epoxy resins. Direct dynamics simulations, at the MP2/6-31+G* level of theory, were used to investigate the decomposition of microcanonical ensembles for this molecule. The Arrhenius A and E_a parameters determined from the direct dynamics simulation are in very good agreement with the TST Arrhenius parameters for the MP2/6-31+G* potential energy surface. The simulation method applied here may be particularly useful for large molecules with a multitude of decomposition pathways and whose transition states may be difficult to determine and have structures that are not readily obvious.

1. INTRODUCTION

Computational chemistry is an important tool for studying unimolecular reactions.[1,2] To understand the dynamics and kinetics of a unimolecular reaction, it is necessary to know the atomic-level mechanism(s) by which a molecule dissociates.[3] Electronic structure calculations[4] are often used to identify the important unimolecular pathways and transition states (TSs). A classical trajectory chemical dynamics simulation[5] may be performed to investigate the molecule's atomistic intramolecular and unimolecular dynamics.[1,2] The potential energy surface (PES) for this simulation may be an analytic potential energy function,[6,7] or the simulation may be performed by direct dynamics,[8,9] in which the gradient and potential energy for calculating the trajectory is obtained directly from an electronic structure theory.

For large molecules and/or high energies (e.g., hyperthermal),[10−12] identifying reaction pathways and TS properties by electronic structure calculations becomes less practical and more challenging. This is because the important decomposition pathways may become less identifiable, and there is the possibility of a multitude of pathways.[13,14] Such effects are found when protonated peptide ions collide with hydrocarbon surfaces.[15,16] For collisions of protonated diglycine with the diamond {111} surface, at a collision energy of 100 eV, 88 different fragmentation pathways of the peptide ion are observed.[15] Similarly, protonated octaglycine dissociates via 304 pathways when it collides with the diamond {111} surface at 100 eV.[16] Identifying TSs for all of these pathways would be a formidable task and may also be impractical.

In this article a classical trajectory direct chemical dynamics simulation procedure is described and applied for determining the reaction pathways of a molecule undergoing unimolecular decomposition at temperature T. Furthermore, by calculating the unimolecular constants $k_i(T)$ for the individual paths versus T, the Arrhenius parameters A and E_a for the paths may be determined. The unimolecular reactions investigated are those for decomposition of $CH_3-NH-CH{=}CH-CH_3$ (Figure 1), which represents an important constituent in the polymer of cross-linked epoxy resins.[17,18] This molecule is small enough that the ab initio TSs may be determined, and thus, Arrhenius parameters may be determined for these TSs using transition-state theory (TST) and compared with the simulation values. This provides a test of the simulation methodology. In the following, the theoretical model and the computational methodology are first described, followed by a presentation of the computational results.

2. THEORETICAL MODEL

The theoretical approach used here is based on the recent finding[19] that for a molecule consisting of s harmonic oscillators the classical Rice−Ramsperger−Kassel−Marcus (RRKM) rate constant:

$$k(E) = \nu\left(\frac{E - E_o}{E}\right)^{s-1} \quad (1)$$

and classical TST rate constant:

$$k(T) = \nu \exp(-E_o/k_B T) \quad (2)$$

become equivalent for large E with $E_o/E \ll 1$ and large $s \approx s - 1$. For s classical harmonic oscillators, the energy and the temperature are related by $E = sk_BT$. Thus, a simulation of the unimolecular decomposition of a microcanonical ensemble at

Received: July 2, 2011
Published: September 19, 2011

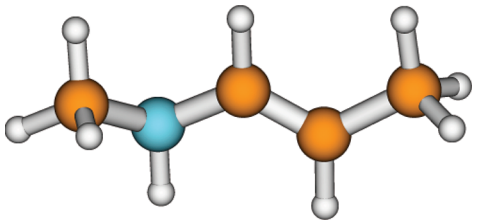

Figure 1. Structure of $CH_3-NH-CH=CH-CH_3$, the molecule investigated for the unimolecular decomposition studies.

energy E may be used to determine the thermal unimolecular rate constant $k(T)$. This relationship is consistent with the understanding that, for a molecule with large s and large E, the populations of the vibrational states of the individual oscillators are given by a Boltzmann distribution[20] and that the fluctuations of the energy of a grand canonical ensemble are negligible, making it similar to a microcanonical ensemble.[21] If anharmonic effects are important, they may be included by multiplying the expressions in eqs 1 and 2 by an anharmonic correction factor,[19] which accounts for anharmonicity in both the reactant molecule and TS.

The trajectories comprising this microcanonical ensemble are integrated until a unimolecular reaction occurs or up to a maximum time t_{max}. The reactions observed are those important for the molecule at temperature T. The total rate constant k for unimolecular decomposition of the molecule may be found by fitting the number of molecules remaining versus time:

$$N(t)/N(0) = \exp(-kt) \quad (3)$$

where $N(0)$ is the number of trajectories for the initial microcanonical ensemble at $t = 0$ or more approximately from the number of trajectories remaining at t_{max}, i.e.:

$$N(t_{max})/N(0) = \exp(-kt_{max}) \quad (4)$$

The total number of products formed at t_{max} is $P(t_{max}) = N(0) - N(t_{max})$. The total unimolecular rate constant is a sum of the rate constants for the individual unimolecular pathways, i.e., $k = \Sigma k_i$, and the rate constant for an individual pathway is simply:

$$k_i = [P_i(t_{max})/P(t_{max})]k \quad (5)$$

where $P_i(t_{max})$ is the number of sets of products formed for path i at t_{max}. The Arrhenius parameters A_i and $E_{a,i}$ for path i are found from the Arrhenius equation $k_i(T) = A_i \exp(-E_{a,i}/k_BT)$ by determining k_i as a function of T.

The above theoretical model assumes the unimolecular dynamics are intrinsically RRKM,[22] so that a microcanonical ensemble of states is maintained as the molecule decomposes. As shown by the simulation results, these dynamics are observed for the molecule studied here $CH_3-NH-CH=CH-CH_3$.

3. COMPUTATIONAL METHODOLOGY

3.1. Direct Dynamics Simulations. The simulations are performed using direct dynamics[8,9] in which the technology of classical trajectory calculations is coupled with electronic structure theory. In this manner, the gradient, energy, and possibly Hessian[23,24] needed to calculate the trajectory come directly from an electronic structure theory, without the need for an analytic potential energy function. To initialize the trajectories, the phase space of the reactant molecule is excited randomly at

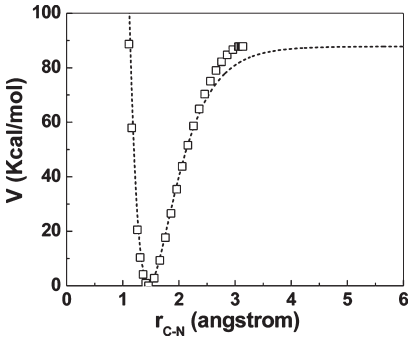

Figure 2. MP2/6-31+G* potential energy curve (□) for $CH_3-NH-CH=CH-CH_3 \rightarrow \cdot CH_3 + \cdot NH-CH=CH-CH_3$ dissociation. The dashed line is the Morse potential energy curve.

fixed energy E to form a microcanonical emsemble.[25] The temperature associated with this energy may be identified from the average kinetic energy of the molecule's N atoms, i.e.:

$$\sum_{i=1}^{N} m_i < v_i^2 > /2 = 3Nk_BT/2 \quad (6)$$

or by equating E to the average thermal energy of the molecule's $s = 3N - 6$ classical oscillators, i.e., $E = sk_BT$. Procedures for forming this microcanonical ensemble are well established.[22,25−29]

The simulations of $CH_3-NH-CH=CH-CH_3$ unimolecular decomposition were performed by exciting microcanonical ensembles of molecules so that their temperatures ($E = sk_BT$) were 3500, 4000, 4500, 5000, and 5500 K. The software package consisting of the chemical dynamics computer program VENUS[30,31] interfaced with the NWChem[32] electronic structure computer program was used for the simulations. A total of 100 trajectories were calculated for each temperature. The simulations were performed by direct dynamics using the MP2/6-31+G* electronic structure theory. The trajectories with T of 3500−5000 K were integrated for t_{max} of 5.1 ps or until a unimolecular reaction occurred. The 5500 K trajectories were integrated with t_{max} = 3.3 ps. The reported uncertainties for the rate constants and the Arrhenius parameters are standard deviations. The temperatures of the simulations were determined from $E = sk_BT$.

3.2. PES and TST Calculations. The model PES for the direct dynamics simulations is given by MP2/6-31+G* theory. It is recognized that MP2 is quite approximate for homolytic bond rupture reactions,[33] due to the shortcomings of Hartree−Fock theory.[34] As discussed below, the most important decomposition pathway found here for $CH_3-NH-CH=CH-CH_3$ is dissociation to $\cdot CH_3 + \cdot NH-CH=CH-CH_3$. The MP2 potential energy curve for this dissociation is given in Figure 2. The potential energy varies from 87.76 kcal/mol at r_{C-N}= 3.06 Å to 87.78 kcal/mol at r_{C-N}= 3.14 Å, with a maximum of 87.83 kcal/mol at 3.11 Å. This dissociation energy is similar to the experimental value of 85.1 kcal/mol for CH_3-NH_2.[35] The CH_3-NH dissociation energy, for the molecule studied here, is expected to be slightly lower than the value for CH_3-NH_2, since replacing one of the H-atoms of $-NH_2$ by a C-atom lowers the bond energy.[35]

The TS for $CH_3-NH-CH=CH-CH_3 \rightarrow \cdot CH_3 + \cdot NH-CH=CH-CH_3$ dissociation is variational, and its structure is determined by the shape of the potential energy curve.[36−38] As shown by earlier work,[39] MP2 theory does not give the correct

dx.doi.org/10.1021/ct200459v |J. Chem. Theory Comput. 2011, 7, 3478–3483

potential energy curve for such a dissociation. Using the MP2 dissociation energy of 87.83 kcal/mol and MP2 quadratic force constant for C−N stretching of 5.20 mdyn/Å, the Morse potential energy curve, $V = D\{1 - \exp-[\beta(r - r_o)]\}^2$, is given in Figure 2, where it is compared with the MP2 potential energy curve. (This C−N stretching force constant is only slightly larger than the experimental value of 5.12 mdyn/Å for CH_3NH_2.)[35] The MP2 curve rises more steeply and may be fit by a *r*-dependent Morse β parameter.[40,41] Such a curve has been referred to as a "stiff" Morse potential.[40,41] The variational TS[42] for a stiff Morse potential is at a much shorter bond length than for the standard Morse potential, resulting in a much "tighter" TS.[42] This leads to a significantly smaller *A* factor for the stiff Morse potential. For $CH_4 \rightarrow H + CH_3$ dissociation, the *A* factor is an order of magnitude smaller for the stiff Morse potential.[40−42] The Morse potential more accurately models the actual potential energy curve than does the "stiff" Morse potential.[39] Thus, the MP2 direct dynamics is expected to give an *A* factor for $CH_3{-}NH{-}CH{=}CH{-}CH_3 \rightarrow \cdot CH_3 + \cdot NH{-}CH{=}CH{-}CH_3$ dissociation, which is significantly smaller than the assumed experimental value of $10^{16}-10^{17}$ s^{-1}.[43]

Classical TST calculations were performed to calculate Arrhenius parameters for the MP2/6-31+G* PES, to compare with the Arrhenius parameters determined from the MP2/6-31+G* direct dynamics simulations. As discussed below, three pathways were considered for this comparison, i.e., the decomposition to $\cdot CH_3 + \cdot NH{-}CH{=}CH{-}CH_3$ and two isomerization reactions. For the harmonic oscillator model, the classical TST rate constant in eq 2 is given by

$$k(T) = \frac{\prod_{i=1}^{s} \nu_i}{\prod_{i=1}^{s-1} \nu_i^{\neq}} \exp(-E_o/k_B T) \qquad (7)$$

where the ν_i are the vibrational frequencies for the unimolecular reaction, the $\nu_i^{\neq}$ the vibrational frequencies for the TS, and E_o the classical potential energy barrier for the MP2 PES. The ratio of the products of vibrational frequencies is the Arrhenius *A* factor and E_o is the activation energy.

The above harmonic oscillator model is expected to be applicable for the two isomerization reactions, which have "tight" transition-state structures located at the isomerization barriers. As discussed above, the C−N dissociation reaction to form $\cdot CH_3 + \cdot NH{-}CH{=}CH{-}CH_3$ has a variational TS located at the minimum in $k(T)$ along the dissociation path.[37,38] For bond dissociations, such as $CH_4 \rightarrow H + CH_3$, a harmonic oscillator variational TST model is accurate,[44−46] and this model is used here for C−N bond dissociation. Vibrational frequencies and potential energies are found along the intrinsic reaction coordinate (IRC),[47,48] and this information is used to find the minimum in $k(T)$, i.e., eq 7. These calculations were performed with the GAMESS computer program.[49]

The IRC frequency for the CH_3 torsion about the C−N bond was found to be unstable, and its value was found by interpolation between the frequency of 208 cm^{-1} at the $CH_3{-}NH{-}CH{=}CH{-}CH_3$ potential energy minimum to 29.8 cm^{-1} at the energy maximum at R_{C-N} = 3.11 Å (see above). In previous work, the frequency for such a mode was found to decay approximately exponentially as the bond ruptures.[39−51] This exponential interpolation, as well as linear interpolation, was considered here and found to give similar results.

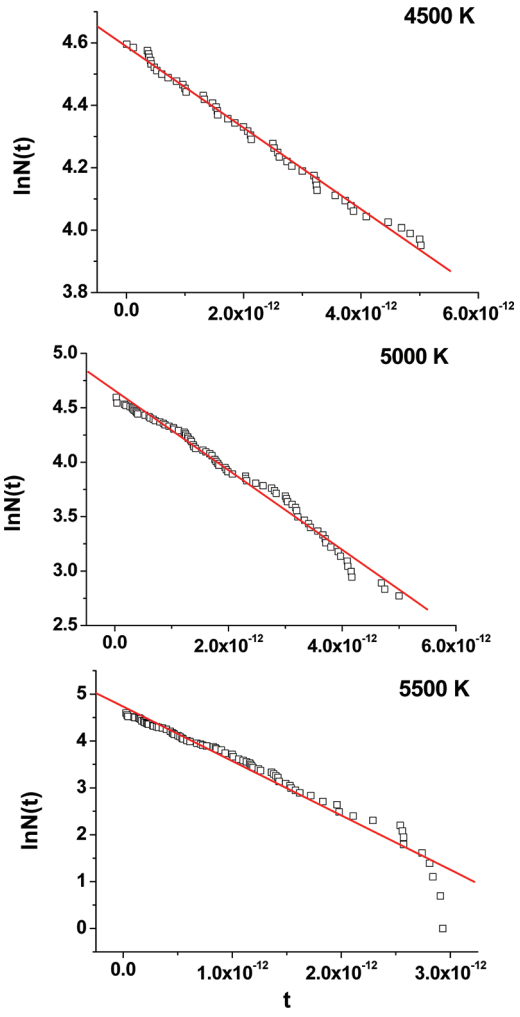

Figure 3. Plots of ln $N(t)$ for the number of excited $CH_3{-}NH{-}CH{=}CH{-}CH_3$ molecules remaining versus time for simulations at 4500, 5000, and 5500 K. The fits are to eq 4. The unit for t is sec.

A more accurate representation of the C−N dissociation reaction may require a flexible variational TST model[52−54] which treats the transitional vibrational modes, that are transformed into product rotations, as hindered rotational degrees of freedom. An important property of the model is that it includes anharmonicity for the transitional modes.[55,56] A possible shortcoming is the assumed separability between the transitional and remaining modes, which becomes more approximate as the length of the rupturing bond is shortened. This could be a problem for the MP2/6-31+G* PES, which has a "stiff" Morse potential for the C−N bond (see above). However, in future analyses of this C−N bond dissociation, it would be of interest to consider the flexible variational TST model.

The TST activation energies and *A* factors for the MP2/6-31+G* PES were compared with these parameters found from the chemical dynamics simulations. The TSs for the isomerization reactions were placed at their potential barriers to give their E_o values and the *A* factors were calculated from eq 7. For C−N dissociation, both the bond dissociation energy and the potential energy at the IRC variational TS were considered as possible MP2 values for E_o. The dissociation *A* factor is that for the variational TS.

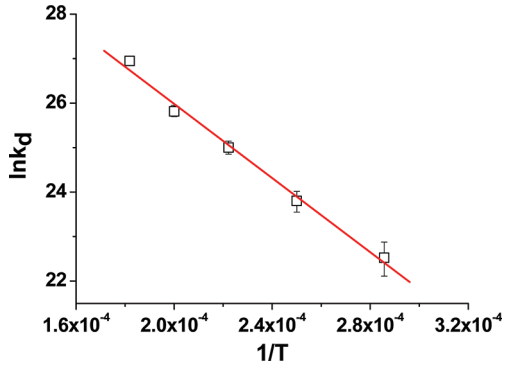

Figure 4. Plot of ln k_d versus $1/T$ for $CH_3-NH-CH=CH-CH_3 \rightarrow \cdot CH_3 + \cdot NH-CH=CH=CH_3$ dissociation. The linear fit yields the Arrhenius parameters E_a = 82.8 ± 4.3 kcal/mol and A = 8.01 + 5.24/−3.17 × 10^{14} s^{-1}. The k_d is in units of s^{-1}, and T is in K.

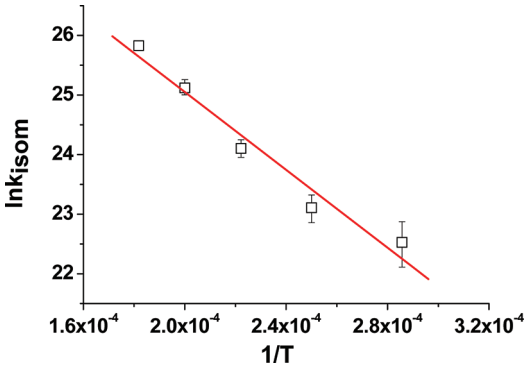

Figure 5. Plot of ln k_{isom} versus $1/T$ for forming the isomerization products $CH_3-N=CH-CH_2-CH_3$ and $CH_3-NH-CH_2-CH=CH_2$. The linear fit yields the Arrhenius parameters E_a = 64.9 ± 7.0 kcal/mol and A = 5.2 + 4.5/−2.8× 10^{13} s^{-1}. The k_{isom} is in units of s^{-1}, and T is in K.

4. SIMULATION RESULTS

A total of 100 trajectories were calculated for each of the temperatures 3500, 4000, 4500, 5000, and 5500 K. The number of trajectories which reacted within t_{max} for the respective temperatures is 6, 19, 48, 84, and 100. A total of 33 different primary and secondary decomposition pathways were observed, and a mechanistic analyses of these pathways and their relationship to experiment will be presented elsewhere.[57] Of interest here is the kinetics analysis discussed in Section 2. The dominant pathway is C−N bond rupture to form the radicals $\cdot CH_3$ and $\cdot NH-CH=CH-CH_3$. The isomerizations via H-atom transfer, to form $CH_3-N=CH-CH_2-CH_3$ and $CH_3-NH-CH_2-CH=CH_2$ are also important pathways. This bond rupture and these isomerizations are considered here.

Using the number of dissociations which occurred within t_{max}, eq 4, the rate constant k for decomposition of $CH_3-NH-CH=CH-CH_3$ is (1.21 +0.49/−0.50) × 10^{10}, (4.13 +0.93/−0.97) × 10^{10}, (1.28 +0.18/−0.20) × 10^{11}, and (3.59 +0.41/−0.51) × 10^{11} s^{-1} for T of 3500, 4000, 4500, and 5000 K, respectively. Equation 4 may not be used to calculate a rate constant for 5500 K, since all the trajectories dissociated within t_{max}. For the calculations at 4500, 5000, and 5500 K, there is a sufficient number of reactions to find the rate constant from a plot of ln $N(t)$ versus t; i.e., eq 3. The plots are given in Figure 3, and the fitted rate constants for the respective temperatures are 1.30 ± 0.02 × 10^{11}, 3.65 ± 0.05 × 10^{11}, and 1.16 ± 0.03 × 10^{12} s^{-1}. Values for these rate constant found from nonlinear fits of eq 3 are nearly the same and 1.37 × 10^{10}, 3.41 × 10^{11}, and 9.75 × 10^{11} s^{-1}, respectively. The rate constants from plots of ln $N(t)$ and $N(t)/N(0)$ are in excellent agreement with those found from the single point $N(t_{max})/N(0)$. In the following analyses, the rate constants for 3500−5000 K are from $N(t_{max})/N(0)$, while the 5500 K value is from the ln $N(t)$ plot.

4.1. $CH_3-NH-CH=CH-CH_3 \rightarrow \cdot CH_3 + \cdot NH-CH=CH-CH_3$ Dissociation. The rate constant versus temperature for C−N bond rupture to form $\cdot CH_3 + \cdot NH-CH=CH-CH_3$ was determined using eq 5, the total rate constant versus temperature and the $P_i(t_{max})/P(t_{max})$ ratio for this decomposition pathway. The resulting k_d rate constants are given in Figure 4 as a plot of ln k_d versus $1/T$. The linear fit to this plot gives E_a = 82.8 ± 4.3 kcal/mol and A = 8.0 + 5.2/−3.2 × 10^{14} s^{-1}. The E_a value of 82.8 kcal/mol is similar to but somewhat lower than the MP2 dissociation energy of 87.83 kcal/mol. This difference is expected from the variational nature of the TS for the C−N bond dissociation pathway.[37,38] As the temperature is increased, the free energy barrier for C−N bond rupture moves to a shorter C−N bond length, resulting in activation energies that are decreased as the temperature is increased[37,38] and are less than the dissociation energy. The direct dynamics A factor of ∼10^{15} s^{-1} is much smaller than the expected experimental value of 10^{16}−10^{17} s^{-1} for CH_3 dissociation.[42,43] Such a result is expected. The MP2/6-31+G* potential for C−N bond rupture, Figure 2, is not sufficiently attractive and, thus, gives rise to a variational TS structure that is "too tight". The result is a small A factor.

As discussed in Section 3.2, a harmonic oscillator model, based on the IRC, was used to find a variational TS for C−N bond rupture at 4000 K. The resulting TS is located at a C−N distance of 2.41 Å, giving rise to a potential energy of 73 kcal/mol and a A factor of 8 × 10^{14} s^{-1}. The A factor is the same as the chemical dynamics value, but the E_o is smaller than that from the dynamics. The harmonic IRC variational TST rate constant is 8.5 × 10^{10} s^{-1} and ∼4 times larger than the dynamics value of 2.2 × 10^{10} s^{-1}. Overall, the TST Arrhenius E_o and A parameters for the MP2/6-31+G* PES are consistent with the values found from the MP2/6-31+G* direct dynamics simulation.

It is worth noting that there are ambiguities in the above variational TST calculation due to substantial changes in vibrational modes as the C−N bond ruptures. The CH_3 torsion about this bond may be a vibration for the reactant, but for a sufficient bond extension, it will become a free rotor. Here it is treated as a vibration for both the reactant and the variational TS. The torsion's partition function at the minimum is 13.4 and 40.6 as a vibration and free rotor, respectively. For the C−N bond dissociation maximum at 3.11 Å (Section 3.2), these respective values are 93.3 and 42.3. Thus, treating the torsion as a free rotor at the variational TS would decrease the TST rate constant. In addition, there are four rocking/bending modes whose frequencies go to zero as the C−N bond breaks. It may be better to treat these modes as hindered rotors, instead of vibrations, as is done by the flexible variational TST.[52−56] However, there are approximations in separating these modes from the remaining modes of the dissociating molecule, and also, the uncertainty in treating the CH_3 torsion of the reactant remains.

4.2. $CH_3-NH-CH=CH-CH_3$ Isomerization Reactions. Rate constants versus temperature were determined, as described above, for the isomerization reactions to form the products

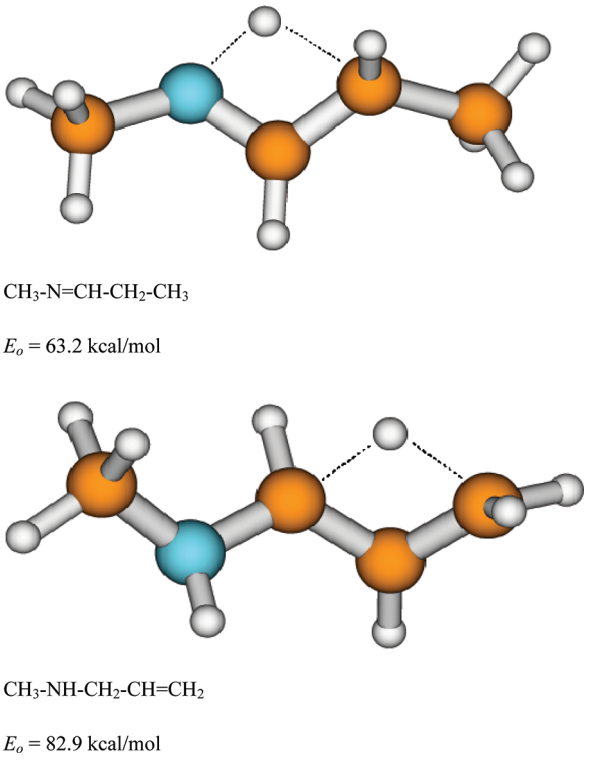

Figure 6. MP2/6-31+G* TS structures and potential energies for forming the isomerization products $CH_3-N{=}CH-CH_2-CH_3$ and $CH_3-NH-CH_2-CH{=}CH_2$.

$CH_3-N{=}CH-CH_2-CH_3$ and $CH_3-NH-CH_2-CH{=}CH_2$. To obtain better statistics, the rate constants for these two pathways were combined to give a total isomerization rate constant k_{isom} versus T. The resulting Arrhenius plot of ln k_{isom} versus $1/T$ is given in Figure 5. The fitted E_a and A are 64.9 ± 7.01 kcal/mol and 5.2 + 4.5/−2.8× 10^{13} s^{-1}.

To compare with these fitted Arrhenius parameters, the ab initio TSs were found for these two isomerizations. Their structures and energies are given in Figure 6. The fitted E_a is intermediate of the two ab initio barrier heights but more akin to E_o = 63.2 kcal/mol for the $CH_3-N{=}CH-CH_2-CH_3$ product. The classical TST A factor, calculated from the reactant molecule and TSs' vibrational frequencies, is 8.8 × 10^{13} s^{-1} for the $CH_3-N{=}CH-CH_2-CH_3$ product and 6.9 × 10^{13} s^{-1} for $CH_3-NH-CH_2-CH{=}CH_2$ product (the latter pathway has a reaction path degeneracy of 3). The fitted A factor is similar to these values. To make a direct comparison with the fitted E_a and A from the chemical dynamics simulation, the classical TST rate constants for the two isomerization paths were summed at each temperature to give a composite rate constant and plotted as ln k_{isom} versus $1/T$. The resulting plot gives E_a = 62.8 kcal/mol and A = 9.2 × 10^{13} s^{-1}, values in overall good agreement with those from the chemical dynamics simulation. That the composite A and E_a are closer to those for the $CH_3-N{=}CH-CH_2-CH_3$ product is consistent with the lower E_a and larger A for this product.

The smaller A factor found from the simulations, as compared to the harmonic TST value, may be the result of anharmonic effects for the chemical dynamics on the MP2/6-31+G* PES. This is consistent with the smaller simulation total isomerization rate constants as compared to those for the TST calculations. For the T of 3500, 4000, 4500, 5000, and 5500 K, the respective simulation rate constants are 5.2 × 10^9, 1.9 × 10^{10}, 5.0 × 10^{10}, 1.2 × 10^{11}, and 1.5 × 10^{11} s^{-1}. The TST values are approximately a factor of 2 larger and 1.1 × 10^{10}, 3.4 × 10^{10}, 8.2 × 10^{10}, 1.7 × 10^{11}, and 3.0 × 10^{11} s^{-1}.

5. CONCLUSIONS

For the work presented here a classical trajectory direct chemical dynamics simulation approach is described for determining unimolecular reaction paths and Arrhenius parameters. This method is expected to be particularly useful for large molecules with many decomposition paths and whose TSs may be difficult to determine by standard electronic structure theory methods. The simulations are performed by coupling the methodology of chemical dynamics simulations with electronic structure theory[8,9] and involve studying the unimolecular decomposition of microcanonical ensembles of molecules.

The molecule studied here is $CH_3-NH-CH{=}CH-CH_3$, an important constituent in the polymer of cross-linked epoxy resins.[17,18] This epoxy resin is a component in flame resistant nanocomposites,[17,58] and it is important to understand its decomposition kinetics at high temperatures, as is done here. Arrhenius parameters for decomposition of $CH_3-NH-CH{=}CH-CH_3$ to $\cdot CH_3 + \cdot NH-CH{=}CH-CH_3$ and isomerization to $CH_3-N{=}CH-CH_2-CH_3$ and $CH_3-NH-CH_2-CH{=}CH_2$ were determined from direct dynamics simulations at the MP2/6-31+G* level of theory. The Arrhenius activation energies determined from the simulation are in good agreement with the isomerization potential energy barriers and C−N bond dissociation energy for the MP2/6-31+G* PES. TST is used to calculate Arrhenius A factors for the MP2/6-31+G* PES, and they are in good agreement with the values found from the simulations. Overall, the TST Arrhenius parameters for the MP2/6-31+G* PES are consistent with the values obtained from the MP2/6-31+G* direct dynamics simulation.

It is pointed out that there are uncertainties and ambiguities in the TST calculations as a result of anharmonic effects and the treatment of modes in the variational TST calculations for C−N bond rupture. A strength of a direct dynamic simulation is that these effects are accurately represented in determining the Arrhenius parameters.

Additional applications and tests of the computational chemistry approach described and applied here, for determining unimolecular decomposition pathways and Arrhenius parameters, are expected. It may be particularly useful for studying nanomaterials and biological molecules.

AUTHOR INFORMATION

Corresponding Author
*E-mail: bill.hase@ttu.edu.

ACKNOWLEDGMENT

This material is based on work supported by the Office of Naval Research under award no. N00014-09-1-0626 and by the Robert A. Welch Foundation under grant no. D-0005. The Hrothgar computer cluster at Texas Tech University, under the direction of the High Performance Computing Center and Philip W. Smith, was used for the simulations reported here.

REFERENCES

(1) Hase, W. L.; Schinke, R. Role of Computational Chemistry in the Development of Unimolecular Rate Theory. In *Theory and Applications of Computational Chemistry: The First 40 Years*; Dykstra, C. E., Frenking, G., Kim, K. S., Scuseria, G., Eds.; Elsevier: New York, 2005, pp 397−423.

(2) Lourderaj, U.; Hase, W. L. *J. Phys. Chem. A* **2009**, *113*, 2236.

(3) Baer, T., Hase, W. L. Unimolecular Reaction Dynamics. *Theory and Experiments*; Oxford: New York, 1996.

(4) Simons, J. *J. Phys. Chem.* **1991**, *95*, 1017.

(5) Bunker, D. L. *Methods Comput. Phys.* **1971**, *10*, 287.

(6) Hase, W. L.; Mrowka, G.; Brudzynski, R. J.; Sloane, C. S. *J. Chem. Phys.* **1978**, *69*, 3548.

(7) Vande Linde, S. R.; Hase, W. L. *J. Phys. Chem.* **1990**, *94*, 2778.

(8) Bolton, K.; Hase, W. L.; Peslherbe, G. H. Direct Dynamics Simulations of Reactive Systems. In *Multidimensional Molecular Dynamics Methods*; Thompson, D. L., Ed. World Scientific Publishing, Inc.: London, 1998; pp 143−189.

(9) Sun, L.; Hase, W. L. *Rev. Comput. Chem.* **2003**, *19*, 79.

(10) Minton, T.; Garton, D. J. Dynamics of Atomic Oxygen Induced Polymer Degradation in Low Earth Orbit. In *Chemical Dynamics in Extreme Environments*, Advanced Series in Physical Chemistry; Dressler, R. A., Ed.; World Scientific Publishing, Inc.: London, 2001; Vol. 11, pp 420−489.

(11) Troya, D.; Schatz, G. C. *Int. Rev. Phys. Chem.* **2004**, *23*, 341.

(12) Yan, T.−Y.; Doubleday, C.; Hase, W. L. *J. Phys. Chem. A* **2004**, *108*, 9863.

(13) Meroueh, S. O.; Wang, Y.; Hase, W. L. *J. Phys. Chem. A* **2002**, *106*, 9983.

(14) Laskin, J.; Futrell, J. H. *J. Am. Soc. Mass Spectrom.* **2003**, *14*, 1340.

(15) Wang, Y.; Hase, W. L .; Song, K. *J. Am. Soc. Mass Spectrom.* **2003**, *14*, 1402.

(16) Park, K.; Deb, B.; Song, K.; Hase, W. L. *J. Am. Soc. Mass Spectrom.* **2009**, *20*, 939.

(17) Tseng, C.−H.; Hsueh, H.−B.; Chen, C.-Y. *Compos. Sci. Technol.* **2007**, *67*, 2350.

(18) Lin, P.−H.; Khare, R. *Macromolecules* **2009**, *42*, 4319.

(19) Lourderaj, U.; McAfee, J. L.; Hase, W. L. *J. Chem. Phys.* **2008**, *129*, 094701.

(20) (a) Baer, T., Hase, W. L. *Unimolecular Reaction Dynamics. Theory and Experiments*; Oxford: New York, 1996; p 328. (b) Park, K.; Engelkemier, J.; Persico, M.; Manikandan, P.; Hase, W. L. *J. Phys. Chem. A* **2011**, *115*, 6603.

(21) McQuarrie, D. A. *Statistical Thermodynamics*; Harper: New York, 1973.

(22) Bunker, D. L.; Hase, W. L. *J. Chem. Phys.* **1973**, *54*, 4621.

(23) Lourderaj, U.; Song, K.; Windus, T. L.; Zhuang, Y.; Hase, W. L. *J. Chem. Phys.* **2007**, *126*, 044105.

(24) Wu, H.; Rahman, M.; Wang, J.; Lourderaj, U.; Hase, W. L.; Zhuang, Y. *J. Chem. Phys.* **2010**, *133*, 074101.

(25) Peslherbe, G. H.; Wang, H.; Hase, W. L. *Adv. Chem. Phys.* **1999**, *105*, 171.

(26) Bunker, D. L. *J. Chem. Phys.* **1962**, *37*, 393.

(27) Hase, W. L.; Buckowski, D. G. *Chem. Phys. Lett.* **1980**, *74*, 284.

(28) Schranz, H. W.; Nordholm, S.; Nyman, G. *J. Chem. Phys.* **1991**, *94*, 1487.

(29) Haile, J. M. *Molecular Dynamics Simulation*; Wiley: New York, 1992.

(30) Hase, W. L.; Duchovic, R. J.; Hu, X.; Domornicki, A.; Lim, K. F.; Lu, D. H.; Peslherbe, G. H.; Swamy, S. R.; Vande Linde, S. R.; Varandas, A.; Wolfe, R. J. *QCPE Bull.* **1996**, *16*, 671.

(31) Hu, X.; Hase, W. L.; Pirraglia, T. *J. Comput. Chem.* **1992**, *12*, 1014–1024.

(32) Bylaska, E. J.; de Jong, W. A.; Govind, N.; Kowalski, K.; Straatsma, T. P.; Valiev, M.; Wang, D.; Apra, E.; Windus, T. L.; Hammond, J.; Nichols, P.; Hirata, S.; Hackler, M. T.; Zhao, Y.; Fan, P.-D.; Harrison, R. J.; Dupuis, M.; Smith, D. M. A.; Nieplocha, J.; Tipparaju, V.; Krishnan, M.; Wu, Q.; Van Voorhis, T.; Auer, A. A.; Nooijen, M.; Brown, E.; Cisneros, G.; Fann, G. I.; Fruchtl, H.; Garza, J.; Hirao, K.; Kendall, R.; Nichols, J. A.; Tsemekhman, K.; Wolinski, K.; Anchell, J.; Bernholdt, D.; Borowski, P.; Clark, T.; Clerc, D.; Dachsel, H.; Deegan, M.; Dyall, K.; Elwood, D.; Glendening, E.; Gutowski, M.; Hess, A.; Jaffe, J.; Johnson, B.; Ju, J.; Kobayashi, R.; Kutteh, R.; Lin, Z.; Littlefield, R.; Long, X.; Meng, B.; Nakajima, T.; Niu, S.; Pollack, L.; Rosing, M.; Sandrone, G.; Stave, M.; Taylor, H.; Thomas, G.; van Lenthe, J.; Wong, A.; Zhang, Z. *NWChem, A Computational Chemistry Package for Parallel Computers*, version 5.1; Pacific Northwest National Laboratory: Richland, WA, 2007.

(33) Duchovic, R. J.; Hase, W. L.; Schlegel, H. B.; Frisch, M. J.; Raghavachari, K. *Chem. Phys. Lett.* **1982**, *89*, 120.

(34) Levine, I. N. *Quantum Chemistry*, 3rd ed.; Allyn and Bacon: Boston, MA, 1973.

(35) *CRC Handbook of Chemistry and Physics*, 89th ed.; Lide, D. R., Ed.; Taylor & Francis Group: Boca Raton, FL, 2008−2009.

(36) Hase, W. L. *J. Chem. Phys.* **1972**, *57*, 730.

(37) Hase, W. L. *J. Chem. Phys.* **1976**, *64*, 2442.

(38) Hase, W. L. *Acc. Chem. Res.* **1983**, *16*, 258.

(39) Hase, W. L.; Mondro, S. L.; Duchovic, R. J.; Hirst, D. M. *J. Am. Chem. Soc.* **1987**, *109*, 2916.

(40) Duchovic, R. J.; Hase, W. L. *Chem. Phys. Lett.* **1984**, *110*, 474.

(41) Duchovic, R. J.; Hase, W. L. *J. Chem. Phys.* **1985**, *82*, 3599.

(42) Hase, W. L.; Duchovic, R. J. *J. Chem. Phys.* **1985**, *83*, 3448.

(43) Johnson, R. L.; Hase, W. L.; Simons, J. W. *J. Chem. Phys.* **1970**, *52*, 3911.

(44) Hu, X.; Hase, W. L. *J. Chem. Phys.* **1991**, *95*, 8073.

(45) Wang, H.; Zhu, L.; Hase, W. L. *J. Phys. Chem.* **1994**, *98*, 1608.

(46) Song, K.; de Sainte Claire, P.; Hase, W. L.; Hass, K. C. *Phys. Rev. B* **1995**, *52*, 2949.

(47) Fukui, k. *J. Phys. Chem.* **1970**, *74*, 4161.

(48) Miller, W. H.; Handy, N. C.; Adams, J. E. J. *Chem. Phys.* **1980**, *72*, 99.

(49) Schmidt, M. W.; Baldridge, K. K.; Boatz, J. A.; Elbert, S. T.; Gordon, M. S.; Jensen, J. H.; Koseki, S.; Matsunaga, N.; Nguyen, K. A.; Su, S.; Windus, T. L.; Dupuis, M.; Montgomery, J. A. *J. Comput. Chem.* **1993**, *14*, 1347.

(50) Hase, W. L. *Chem. Phys. Lett.* **1987**, *139*, 389.

(51) Hu, X.; Hase, W. L. *J. Phys. Chem.* **1989**, *93*, 4029.

(52) Wardlaw, D. M.; Marcus, R. A. *Adv. Chem. Phys.* **1987**, *70*, 231.

(53) Hase, W. L.; Wardlaw, D. M. *Bimolecular Collisions*; Ashfold, M. N. R.; Baggott, J. E., Eds.; Royal Society of Chemistry: London, 1989, p 171.

(54) Klippenstein, S. J. *J. Chem. Phys.* **1992**, *96*, 367.

(55) Klippenstein, S. J.; Georgievskii, Y.; Harding, L. B. *Phys. Chem. Chem. Phys.* **2006**, *8*, 1133.

(56) Harding, L. B.; Georgievskii, Y.; Klippenstein, S. J. *J. Phys. Chem. A* **2005**, *109*, 4646.

(57) Yang, L.; Hase, W. L., to be submitted for publication.

(58) Levchik, S. V.; Weil, E. D. *Polym. Int.* **2004**, *53*, 1901.